Scientific Reports

https://doi.org/10.1038/s41598-025-33002-w

Article in Press

Experimental and numerical analysis of shear behaviour at the interface geopolymer mortar and sand

Received: 5 August 2025

Accepted: 15 December 2025

Published online: 31 January 2026

Cite this article as: Bayındır F., Ekinci E., Sarıcı T. *et al.* Experimental and numerical analysis of shear behaviour at the interface geopolymer mortar and sand. *Sci Rep* (2025). https://doi.org/10.1038/s41598-025-33002-w

Furkan Bayındır, Enes Ekinci, Talha Sarıcı & Alper Özmen

We are providing an unedited version of this manuscript to give early access to its findings. Before final publication, the manuscript will undergo further editing. Please note there may be errors present which affect the content, and all legal disclaimers apply.

If this paper is publishing under a Transparent Peer Review model then Peer Review reports will publish with the final article.

ARTICLE IN PRESS

© The Author(s) 2025. **Open Access** This article is licensed under a Creative Commons Attribution-NonCommercial-NoDerivatives 4.0 International License, which permits any non-commercial use, sharing, distribution and reproduction in any medium or format, as long as you give appropriate credit to the original author(s) and the source, provide a link to the Creative Commons licence, and indicate if you modified the licensed material. You do not have permission under this licence to share adapted material derived from this article or parts of it. The images or other third party material in this article are included in the article's Creative Commons licence, unless indicated otherwise in a credit line to the material. If material is not included in the article's Creative Commons licence and your intended use is not permitted by statutory regulation or exceeds the permitted use, you will need to obtain permission directly from the copyright holder. To view a copy of this licence, visit http://creativecommons.org/licenses/by-nc-nd/4.0/.

ARTICLE IN PRESS

Experimental and Numerical Analysis of Shear Behaviour at the Interface Geopolymer Mortar and Sand

Furkan Bayındır[1], Enes Ekinci[1*], Talha Sarıcı[1], Alper Özmen[1]

[1]Department of Civil Engineering, Inonu University, Malatya, Turkey

Corresponding Author: enes.ekinci@inonu.edu.tr

ABSTRACT

This study aimed to examine the impact of various production parameters on the shear performance at the interface between geopolymer mortar (GPM) and sand soil. Initially, the effects of varying NaOH concentrations (5, 10 and 15M), aggregate types (stream aggregates (SA), crushed stone aggregates (CS) and construction and demolition waste (CDW) aggregates) and alkali/binder ratios (0.5 and 0.6) on GBFS-based GPM specimens were investigated. For this purpose, compressive strength, water absorption and ultrasonic pulse velocity (UPV) tests were carried out on GPM samples cured for 28 days. The maximum 28-day compressive strength (43.6 MPa) and the minimum water absorption (3.78%) were observed in GPM specimens activated with 15 M NaOH, produced with CS, water-cured and cast at an alkali/binder ratio of 0.5. Experimental findings revealed that the effects of aggregate type on high mechanical and low permeability properties were graded as CS> SA > CDW. Additionally, UPV test results showed positive correlation with compressive strength and water absorption values. Subsequently, the shear performance between GPM and sand soil were determined by using shear box test. In direct shear experiments, decreasing the alkali/binder ratio from 0.6 to 0.5 and the usage of CS increased the sand–GPM friction angle. Moreover, numerical modelling was employed to analysed soil-GPM interaction using the finite element method (FEM) in ABAQUS. FEM results showed that the obtained numerical findings demonstrated strong consistency with experimental data, capturing force-displacement trends therefore the numerical model can be used for parametric studies.

ARTICLE IN PRESS

Keywords: Geopolymer; Compressive strength; Shear box; Finite element method, Shear behaviour; UPV analysis

1. Introduction

Traditional concrete remains the premier building material worldwide, owing to its superior characteristics. Its widespread adoption is arised from have validity to international standards, superior mechanical performance, local resource availability, and cost-effectiveness [1, 2, 3]. These important features have caused the demand for concrete to increase continuously and the production of cement in very high quantities [4]. A previous study indicated that the Portland cement industry achieved a yearly production volume of around 4 billion tons, with a growth rate of 4% [5]. Furthermore, other studies highlighted that producing 1 ton of Portland cement can release about 0.8 ton of CO_2 into the atmosphere [6], and the cement manufacturing industry accounts for nearly 7% of global CO_2 emissions [7]. In addition to air pollution caused by CO_2 emissions during cement production, it was also reported that further adverse environmental impacts, including noise pollution [8] and water contamination from dust generation [9]. These environmental effects reveal that the chance given to cement, which has been used for over 200 years, must come to an end and that eco-friendly building materials that can be an alternative to cement must be used. Of course, the construction and building sector is not the only sector that has negative effects on the environment. Industrial activities that serve many different purposes also have quite severe effects on the environment by generating substantial amounts of waste materials [10]. Geopolymer binders, the most promising alternative to conventional Portland cement, were first introduced by Davidovits [11]. Geopolymer composites produced from the alkali activation of industrial secondary products or natural resources are notable for their exceptional durability properties, superior compressive strength and reduced environmental footprint [12]. Many different successful studies such as high strength concrete production [13], lightweight [14] concrete production, self-

ARTICLE IN PRESS

compacting concrete production [15] and soil stabilization [16-18] were carried out on geopolymer composites with these unique properties and promising findings were obtained. However, the production parameters of geopolymer composites that have not yet been standardized indicate that their use in different applications is only possible with the application of a very extensive experimental process. For instance, Geçkil et al. (2025) investigated the feasibility of CDW and FA-based geopolymers in soil stabilization. Experimental findings indicated that CDW could be a significant alternative to natural aggregates as a filler material when reacted with alkali activators [17]. Furthermore, in another study examining the effects of blast furnace slag addition on soil stabilization, Sarici et al. (2025) reported that CDW aggregates with 20% blast furnace slag added increased their ultimate bearing capacity by up to 4.72 times compared to samples without additives [18]. Unlike these soil-stabilization studies, this study quantifies difference in mechanical and physical properties of GPM specimens by conducting a systematic optimization along with different parameters. It directly demonstrates its impact on the shear behavior at the sand-GPM interface using shear data and calibrates and validates this relationship with a FEM-based model.

The shear behaviour of soil-structure interfaces is the determinant of load transfer and deformation formation in a large number of civil engineering structures, from pile foundations to retaining walls. In concrete or cementitious hybrid piles, which are commonly employed as a ground improvement method due to their high bearing capacity and low settlement characteristics, most of the vertical loads are transmitted by shear resistance on the soil-concrete contact surface [19]. Interface friction also plays a critical role in systems such as retaining walls, tunnel linings, building foundations, channels, geosynthetic reinforced fillings, seepage barriers, piles, etc. There are various regulations for the determination of soil-structure interface friction characteristics, but these regulations may not give realistic results for practical applications when designing [20, 21].

ARTICLE IN PRESS

Zohra et al. (2022) comprehensively discussed the mechanical behaviour of the interface in their study. In their study, they explained the importance of interface behaviour in engineering, shear test methods in laboratories, mechanical models used to describe the interface, approaches to represent the contact between soil and structure with finite elements, mechanisms such as effective friction at the interface, cohesion effect, roughness effect, stress-strain relationships, shear band formation, surface deformations, etc. They also presented predicted needs and recommendations for future research [22]. In a study conducted by Tee and Mostofizadeh (2024), the nonlinear behavior of soil and geopolymer concrete pipes was investigated using a software package. They conducted static and dynamic analyses. They found that soil density was the most influential parameter in both static and dynamic scenarios. They stated that this result will help us understand the complex behavior of underground concrete pipes, especially during earthquake events [23]. This study demonstrates the importance of determining the shear behavior of the soil-geopolymer concrete interface. Haeri et al. (2019) investigated the effects of surface roughness and vertical normal stress on the shear behavior at the interface of a cohesive soil and concrete using direct shear tests on two-layered specimens prepared in the laboratory. They created the interface roughness with one or two teeth and 15° or 30° angles in both the soil and concrete. They found that the failure mode is generally sensitive to normal stress and roughness. At low normal stresses, the teeth sheared and slipped from the base, while at high stresses, they observed separation with oblique cracks. They also reported that shear strength depends on the tooth geometry. Consequently, they concluded that the shape/number of roughness and the normal stress level significantly control the interface shear capacity at the in-situ or precast concrete-soil contact surfaces [24].

Non-linear contact behaviour in the interface zone under various loadings depends on various factors and these contact behaviours have various effects. These mechanisms depend on the behaviour of the soil and the construction material themselves and the stress-strain relationship at their joint contact. Indeed, the interface is defined as the joint working surface

ARTICLE IN PRESS

where the soil and the construction material transfer force to each other. Understanding the material interaction in this region is essential for design criteria such as bearing capacity, deformation, seismic behaviour, etc. In the interface zone, the part of the soil in close contact may behave differently from the main soil deposit. Therefore, the concept of a “close contact interface zone”, where the soil in direct contact with the structure can acquire a special formation, should be considered. This thin layer may differ from the surrounding soil in terms of shear strength parameters, degree of compaction, grain pattern and water content and can significantly affect soil-structure interaction [19-22].

Li et al. (2022) conducted a study to examine the effect of various soil types, moisture contents and interlayer materials (sand-silt) on shear parameters at soil-concrete interfaces using a large-scale test set-up. They reported that shear stress increased with displacement in the first phases and then stabilized, but stabilization was reached at smaller displacement in sandy soil. They reported that thin interlayer (filling) applications with fine sand or silt had limited influence on the total shear strength of the interface but created different directional changes in friction angle and cohesion. They observed that the friction coefficient at the medium-coarse sand–concrete interface was greater than that at the silty sand–concrete interface. It was also attributed this behaviour the presence of voids between large particles as well as between soil particles and concrete leading to the embedding effect and improving the interfacial coefficient of friction [25]. Janipour et al. (2022) investigated the effects of relative density, surface roughness of concrete, normal stress and shear zone surface ratio on the shear strength of sand-concrete contact surface. They stated that when they increased the concrete surface roughness by making grooves, the internal friction angle they determined for the sand-concrete contact surface also increased. According to the results obtained in their study, they stated that roughness depth and sand density have a significant effect on interface friction [20]. Li et al. (2022) investigated the shear behaviour of cement-stabilized soil-concrete interfaces by direct shear tests. They investigated the effect of cement dosage and normal stress variables on the shear stress-

ARTICLE IN PRESS

displacement relationship and found that the stress increases approximately linearly in the initial phases, then decreases sharply to the residual stress level when the bond strength is reached. They reported that the peak stress is relatively insensitive to normal stress, while the residual stress increases significantly, especially at high normal stresses [19].

The literature on the shear behaviour of soil-concrete interfaces has shown that studies in the field of soil-structure interaction interfaces combine the knowledge of soil behaviour, which is the foundation of geotechnical engineering, with structural materials and contact mechanics. As the scientific understanding of this interface improves and more detailed studies on these topics are conducted, safer and more economical designs will be possible. This will lead to advances such as more realistic assessment of the bearing capacity of pile foundations (especially friction piles), more realistic optimization of surface coatings in tunnel segments, development of innovative interface materials for soil stabilization, etc. Also, successful modelling of interface behaviour requires calibration based on accurate experimental data, appropriate model selection and a holistic understanding of the mechanisms.

ARTICLE IN PRESS

Determining the interactions between soil and concrete are an essential aspect of geotechnical engineering, affecting the efficacy of constructions. The first method of determination that comes to mind is experimental. However precise numerical modelling of this interaction is crucial for comprehending shear behaviour and enhancing design tactics. The finite element method (FEM) serves as an effective instrument for simulating these interactions, facilitating a comprehensive evaluation of stress distributions, deformations, and failure causes. Several research have employed direct shear box testing and numerical simulations to elucidate the shear resistance processes at the contact. Medzvieckas et al. (2019) examined the distribution of vertical stresses in direct shear testing utilizing PLAXIS 3D, emphasizing the influence of dilatation on stress redistribution [26]. Dastgerdi et al. (2024) examined the effect of shear box geometry on stress distribution, concluding that circular shear boxes

ARTICLE IN PRESS

provide more uniform stress distributions than square shear boxes. Multiple researchers have investigated the influence of interface characteristics on numerical simulations [27]. Moayed et al. (2012) using the modified Drucker-Prager model to predict the behaviour of sandy clay, illustrating the impact of modifications in cohesion and friction angle on shear strength [28]. Aas (2023) utilized ABAQUS to simulate direct shear testing on rock joints, highlighting the significance of asperity interlocking in ascertaining joint shear strength [29]. Additionally, Zhan et al. (2012) and Qian et al. (2017) applied the Mohr-Coulomb failure criterion to model soil-structure interactions, reinforcing the importance of selecting appropriate material models in finite element analyses [30, 31]. Similarly, Tu et al. (2025) validate a 3-D DEM model of soil-rock mixtures using lab tests. Square shear boxes yielded more accurate parameters than circular boxes, which overestimated the cohesion (+7%) and friction angle (+5%). Reducing the shear-box length-to-width ratio (L/W) shifts the behavior from strain-softening (L/W≥1:1) to strain-hardening (L/W<1:1). Square boxes with L/W=1:1 are optimal; L/W>1:1 gives acceptable errors (≤5%), while L/W<1:1 overestimates the strength by ~15% [32]. The literature indicates that numerical modelling is an essential instrument for comprehending soil-concrete interactions. Discrepancies between experimental and numerical results underscore the necessity for enhanced material models that more accurately represent the intricacies of soil behaviour.

This study aims to investigate the shear behavior at the interface between geopolymer mortar and sand soil, considering various production parameters. In addition, numerical modeling is integrated to validate the experimental findings and provide a basis for future parametric analyses. In summary, it is considered that this study will provide a novel contribution to the literature by revealing the synergistic effects of NaOH concentration, aggregate type, alkali/binder ratio, and curing conditions on the shear behavior at the geopolymer mortar–sand soil interface, supported by both experimental investigations and numerical modelling.

ARTICLE IN PRESS

2. Materials and Methods

2.1. Materials

In this study, GPM specimens were produced using GBFS as binder. There are varied reasons for using GBFS as a binder in the study. The first of these is that the full capacity steel production in Türkiye is approximately 50 million tons per year. Considering that 15-20% of the total production is released as slag in the iron and steel production process, it is particularly important to effectively recycle this by-product [33]. The second reason is that GBFS has the appropriate chemical composition and physical properties required for the geopolymerization reaction. Thermal curing, which is considered to be one of the most important disadvantages of fly ash or metakaolin-based geopolymer binders, is not necessary in BFS-based geopolymer composites. The higher hydration modulus [(CaO+ $MgO+Al_2O_3)/SiO_2$], which provides high mechanical properties with curing technique under ambient conditions, is quite high in GBFS compared to fly ash and metakaolin [34]. Therefore, GBFS has emerged as the most logical choice for applications requiring curing under ambient conditions. The

ARTICLE IN PRESS

GBFS used in the study is presented in Fig. 1, and the chemical characteristics of GBFS are given in Table 1.

Table 1. Chemical characteristics of GBFS

Composition, (%)	SiO_2	CaO	MgO	Al_2O_3	Fe_2O_3	TiO_2	K_2O	Na_2O	SO_3	Mn_2O_3	Cl^-
GBFS	32.47	32.45	9.31	9.94	1.25	1.16	0.85	0.31	0.82	3.51	0.015



Fig. 1. GBFS

In this study, alkaline activation of the produced GPM samples was carried out using NaOH solution. To examine the effect of the alkali activator on the properties of the GPM samples, NaOH prepared at three different concentrations (5M, 10M and 15M) is given in Fig. 2. The chemical and physical features of NaOH are given in Table 2.

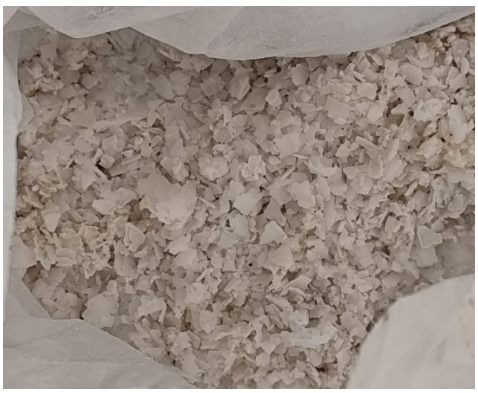


Fig. 2. NaOH

Table 2. Physical and chemical features of NaOH

Properties	NaOH

ARTICLE IN PRESS

Molecular mass, (g/mol)	40.00
Colour	White
pH	13-14
Density, (g/cm^3)	2.13

To investigate the impact of different aggregate types on the mechanical and permeability properties of GPM samples, stream aggregate (SA), crushed stone aggregate (CS) and construction and demolition waste aggregates (CDW) were used. Different types of aggregates used in the study are given in Fig. 3.



a) Steam aggregate **b)** Crushed stone aggregate **c)** CDW

Fig. 3. Different aggregates used in this study

In the shear box experiments, the weak soil deposit was created using sand. The image of the sand is given in Fig. 4. The engineering properties of the sand soil used in this study were determined by experimental studies. According to Unified Soil Classification System (ASTM-D4287), the sand soil utilized was identified as poorly graded sand (SP). The grain diameter distribution of the sand obtained after the sieve analysis test is presented in Fig. 5. In addition, the engineering properties of sand are shown in Table 3.



Fig. 4. Image of the sand soil

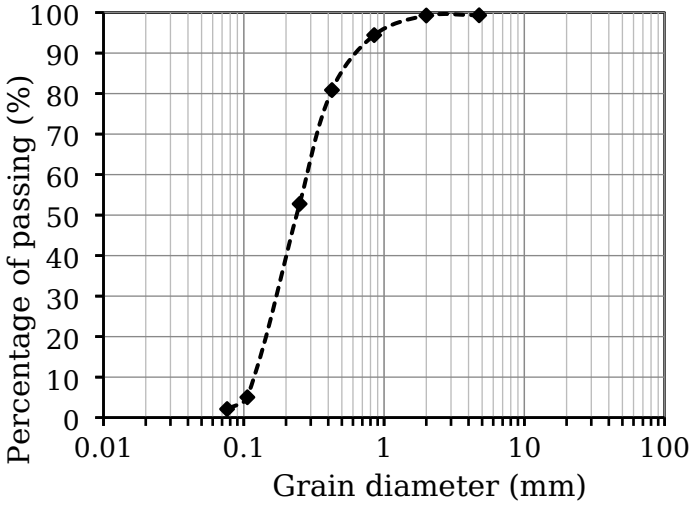


Fig. 5. Grain diameter distribution curve of the sand soil, [30]

ARTICLE IN

Table. 3. Engineering properties of the sand soil, [35]

Properties	Values	Standards
Grain Density	27.5 kN/m^3	ASTM-D854

ARTICLE IN PRESS

Maximum Dry Unit Volume Weight	16.6 kN/m^3	ASTM-D4254
Minimum Dry Unit Volume Weight	14.5 kN/m^3	ASTM-D4254
Uniformity Coefficient	2.38	ASTM-D422
Coefficient of Curvature	0.93	ASTM-D422
Classification	SP	ASTM-D4287
CBR value	5%	ASTM D1883-21
Internal friction angle	37°	ASTM-D3080

2.2. Experimental Procedure

2.2.1. Preparation of GPM samples

Mix proportions of 36 different groups of GPM samples produced by applying three different NaOH concentrations (5M, 10M and 15M), two different alkali/binder ratios (0.5 and 0.6), three different aggregate types (SA, CS, CDW) and two different curing regimes (ambient conditions and water) are given in Table 4. The fresh geopolymer mortar mixture was mixed for 5 minutes and then poured into steel cube molds with dimensions of 50x50x50 mm^3 and molds with dimensions of 60x60x10 mm^3. The GPM specimens were demolded after 24 hours and subsequently were cured for 28 days under laboratory conditions and in water. Images of the molds used in the study are given in Fig. 6. Additionally, the flow diagram of the study design is presented in Fig.7.

ARTICLE IN PRESS

Table 4. Mix proportions of GPM specimens

	NaOH, (g)	**Alkali /**	**Aggregate, (g)**	**Curing Regime**

ARTICLE IN PRESS

Group	GBFS,	5M	10M	15M	0,5	0,6	SA	CS	CDW	Ambient	Water
1	1000	500			✓		2000			✓	
2	1000		500		✓		2000			✓	
3	1000			500	✓		2000			✓	
4	1000	500			✓			2000		✓	
5	1000		500		✓			2000		✓	
6	1000			500	✓			2000		✓	
7	1000	500			✓				2000	✓	
8	1000		500		✓				2000	✓	
9	1000			500	✓				2000	✓	
10	1000	600				✓	200			✓	
11	1000		600			✓	200			✓	
12	1000			600		✓	200			✓	
13	1000	600				✓		200		✓	
14	1000		600			✓		200		✓	
15	1000			600		✓		200		✓	
16	1000	600				✓			200	✓	
17	1000		600			✓			200	✓	
18	1000			600		✓			200	✓	
19	1000	500			✓		2000				✓
20	1000		500		✓		2000				✓
21	1000			500	✓		2000				✓
22	1000	500			✓			2000			✓
23	1000		500		✓			2000			✓
24	1000			500	✓			2000			✓
25	1000	500			✓				2000		✓
26	1000		500		✓				2000		✓
27	1000			500	✓				2000		✓
28	1000	600				✓	200				✓
29	1000		600			✓	200				✓
30	1000			600		✓	200				✓
31	1000	600				✓		200			✓
32	1000		600			✓		200			✓
33	1000			600		✓		200			✓
34	1000	600				✓			200		✓
35	1000		600			✓			200		✓
36	1000			600		✓			200		✓

ARTICLE IN PRESS

ARTICLE IN PRESS

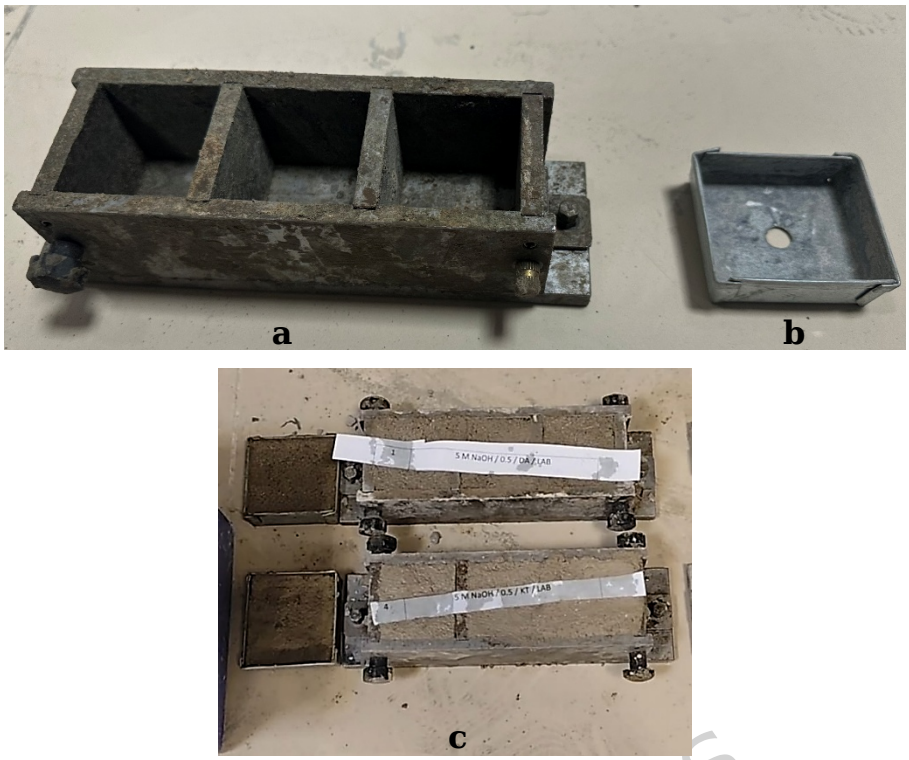


Fig. 6. Moulds used in this study: (a) three-cell steel cube mould (50x50x50 mm^3) for compressive strength/UPV specimens; (b) stainless-steel mould (60×60x10 mm^3) for direct-shear specimens; (c) Casting fresh GPMs into moulds

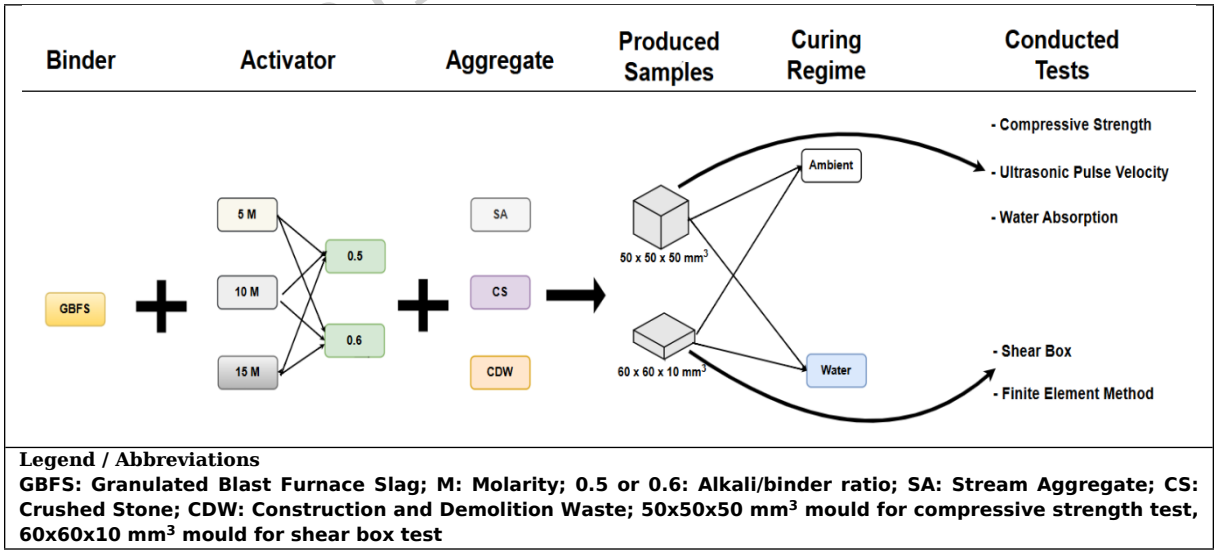


Fig. 7. Experimental flowchart of sample preparation and testing program

ARTICLE IN PRESS

28-day compressive strength were conducted in compliance with ASTM C109 standard [36]. As seen in Fig. 8, ultrasonic pulse velocity (UPV) measurements were taken from the smooth opposite faces of the cube samples, perpendicular to the concrete casting direction. In order to ensure full contact between the sensors and the surfaces to be measured, the surfaces were first cleaned of dust and then gel was applied and measurements were taken.



Fig. 8. UPV experiment

The oven dry (W_k), saturated (W_d) and weight in water (W_s) values of geopolymer mortar samples were obtained and the water absorption values of GPM specimens were recorded with the help of the equation given below in accordance with ASTM C 642-06 (2013) [37].

$$\Omega = (W_D - W_K) / W_K \times 100 \quad (1)$$

where: "Ω" represents the water absorption value.

2.2.2. Shear Box Tests

The shear box test was conducted in a 60x60x10 mm^3 test box. The shear box test setup is given in Fig. 9. Shear box tests were conducted as described in the literature [19-22] and ASTM D3080 standard [38]. The tests started with fixing the prefabricated geopolymer mortar slab to the lower shear box. In the upper box, the sand soil was poured from a certain height in layers to reach the target relative density (Dr=35%) and each layer was compacted with very light vibrations. To check whether the sand has reached the desired relative density, the density value was checked

using volume and mass values. Thus, a loose sand soil deposit was created on the geopolymer mortar and the sand-geopolymer mortar contact was ensured to be homogeneous. Then, one of the normal stresses (σ_n = 27.2, 54.5 and 109 kPa) was applied sequentially. Consolidation was considered complete when the volume change stopped while the normal stress was applied. Then, during the shear stage, the upper box was moved horizontally at a constant speed of 1 mm/min while the lower box was stationary, during which the load cell continuously recorded the horizontal force and the LVDT sensors continuously recorded the horizontal and, if present, vertical displacements. The peak shear stress (τ_p) and the displacement value occurring at this stress were determined from the stress-displacement curve resulting from the experiment. Using τ_p values for each normal stress level, the Mohr-Coulomb equation was utilized for calculating the angle of internal friction at the sand-geopolymer mortar interface: $\delta = \arctan(\tau_p/\sigma_n)$.

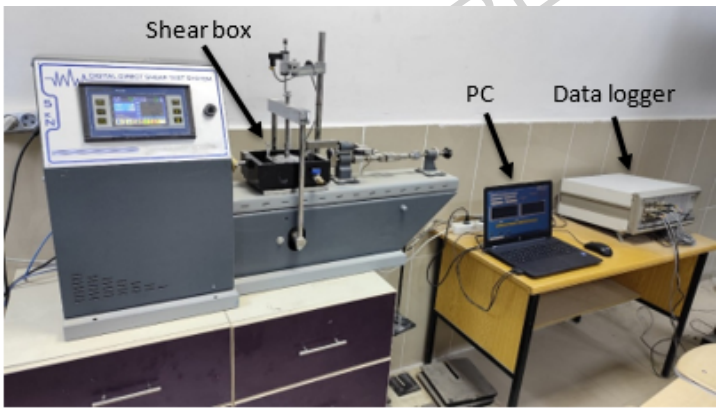


Fig. 9. Shear box test set-up

2.3. Finite Element Modelling of the Shear Box Tests

The soil-concrete interface is a common engineering problem in engineering structures and is critical for shear resistance. The interaction between soil and concrete significantly affects the performance of various structural components such as pile foundations, retaining walls, and tunnel linings. In this section of the study, the friction behaviour at the soil-GPM interface was numerically modelled using the finite element method (FEM). In the analyses ABAQUS finite element software was used. In the modelling of the shear box experiment, the geometric properties of the

ARTICLE IN PRESS

actual experimental set were used. Accordingly, the soil medium has been modelled with dimensions of 60x60x25 mm, and the GPM medium with dimensions of 60x60x10 mm. The analysis consists of 2 stages. First, a uniform normal force was applied to the model, and then a lateral displacement was applied. In the FEM, the GPM element was placed at the bottom and the ground medium at the top. All surfaces of the GPM element are constrained against movement, while the lateral surfaces of the upper element are constrained in the direction of their normal. The boundary conditions applied in the model are presented in Fig. 10(a), the finite element discretization is shown in Fig. 10(b) and boundary conditions of the model is given in Fig 10(c).

ARTICLE IN PRESS

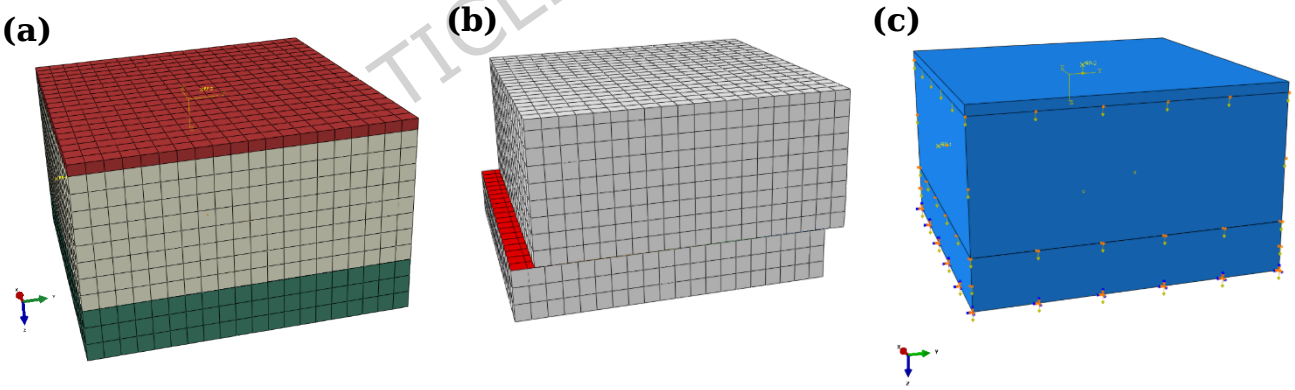


Fig 10. Finite element discretization (a) mesh sensitivity, (b) Working principle, (c) Boundary conditions

In the FEM, the soil layer and GPM materials have been defined as two separate regions. The soil characterized by the Mohr-Coulomb material model is 25 mm thick, and the GPM characterized by the linear elastic material model is 10 mm thick. The Mohr-Coulomb material model, which has been used in many studies [30, 39, 40] to model the nonlinear behaviour of the soil, has been employed. The behaviour of the Mohr-

ARTICLE IN PRESS

Coulomb material model under load is shown in Fig. 11. The Mohr-Coulomb model is a widely used material model in geotechnical engineering, typically employed to represent the behaviour of cohesive and non-cohesive soils. In the ABAQUS software, this model is applied to analyse the plastic deformations and stress-strain behaviour of soils. The Mohr-Coulomb model is based on the relationship between shear stress (τ) and normal stress (σ_n) for material strength:

$$\tau = c + \sigma_n \tan\phi \quad (3)$$

In the Eq. (3), cohesion (Pa), internal friction angle (°), and normal stress (Pa). This model is used to describe both the elastic and plastic behaviour of the material. While the elastic region is defined according to Hooke's law, the plastic region is governed by the Mohr-Coulomb failure criterion and yield rules.

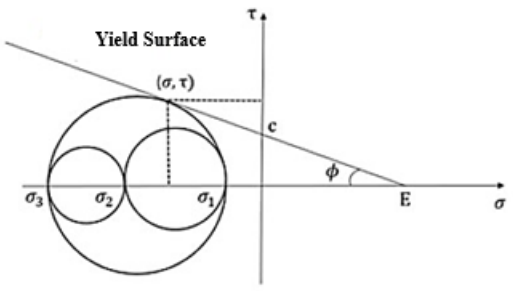


Fig. 11. Mohr coulomb failure criterion [26].

The FEM consists of 4800 3D solid elements and 6174 nodes. The C3D8R element, characterized by 8 nodes, was employed as the solid element. Geopolymer mortar (GPM) parameters were adopted from the literature for ambient-cured GGBS- based geopolymer mortars with comparable activator chemistry and mixture proportions. In particular, the elastic modulus was set to E≈30GPa, consistent with reported ranges for ambient-cured GGBS systems; the hardened density was taken as ρ≈2400kg/m3; and Poisson's ratio was assumed as ν= 0.25, within commonly cited bounds for geopolymer mortars [41-44]. These selections were made to reflect representative behavior under the modeling assumptions used herein."

ARTICLE IN PRESS

The material properties of the materials used in the FEM are given in Table 5.

Table 5. Material properties used in the FEM

Properties	Experimental (Soil)	Numerical model (Soil)	GPM
E (kN/m^2)	12750	13000	30e^6
Density (kN/m^3)	14	14	24
Poisson ratio	0.3	0.3	0.25
C (MPa)	-	0.008	-
Internal friction (^{o})	42	42	-
Dilatancy angle (^{o})	12	12	-

ARTICLE IN PRESS

The contact interface between the two materials has been comprehensively characterized in terms of both shear and normal properties. Sliding Behaviour: To characterize the friction behaviour, static and kinetic friction coefficients have been determined, and an exponential decay model has been applied between these coefficients. This model shows the transition where the static friction coefficient decreases exponentially to the kinetic friction coefficient using the Eq. 4.

$$\mu(v) = \mu_k + (\mu_s - \mu_k)\exp(-c \cdot v) \quad (4)$$

Here, $\mu(v)$ the friction coefficient, μ_s static friction coefficient, μ_k kinetic friction coefficient, c exponential decay coefficient, and v slip speed are present. This approach more realistically reflects how the friction coefficient changes with slip velocity and enables more accurate results, especially in dynamic analyses. Additionally, the elastic shear parameter has also been defined. This parameter allows for the modelling of small relative movements between contact surfaces and simulates the micro-movements of the surfaces before they enter a full sliding state.

ARTICLE IN PRESS

Normal Behaviour: A linear contact stiffness has been used to characterize the contact behaviour in the normal direction. This method is suitable for regulating surface penetration and evaluating the stiffness in the normal direction of contact. Linear contact stiffness indicates the direct relationship between the normal force of the contact surfaces and the normal displacement, serving as a vital criterion for maintaining contact stability. Parameters are defined when specifying contact interaction properties in the ABAQUS program.
Different friction coefficients were considered to simulate the friction behaviour of each sample. By changing the friction coefficients, a sensitivity analysis was conducted, and the numerical models were matched with the experimental data. The creep interface parameters used in the modelling of each sample are provided in Table 6.

Table 6. Interface parameters

Parameter	Tangential behaviour			Normal behaviour
	Static coefficient	Kinetic coefficient	Decay coefficient	Contact stiffness
Model 1	0.93	0.83	0.001	0.014
Model 4	0.75	0.74	0.001	0.01
Model 5	0.83	0.79	0.0015	0.02

ARTICLE IN PRESS

ARTICLE IN PRESS

3. Results and Discussion

3.1. Compressive strength of GPM samples

3.1.1. Effect of aggregate type on compressive strength

Fig. 12 presents the effects of three different aggregate types used for producing GPM samples on the compressive strength values. As seen in Fig. 12, the use of crushed stone (CS) aggregates in almost all geopolymer mortar samples led to significantly superior compressive strength values compared to other aggregate types. This was likely due to the irregular shape of the CS particles, which help improve the adherence between the aggregate and the geopolymer matrix, particularly at the interfacial transition zone. On the other hand, in the sample groups where CDW aggregates were used, comparatively lower compressive strength results were recorded. In the samples where CDW was used, the highest compressive strength was obtained as 31.3 MPa from the 28th group samples activated using 5M NaOH, produced at 0.6 alkali/binder ratio and cured in water. This result shows that obtaining high mechanical performance in GPM specimens produced using CDW as aggregate can be possible with the use of higher liquid ratios. Because CDW aggregates have irregular shapes and high water absorption properties, they affect the workability of the samples quite negatively and reduces the compressive strength values. Similarly, the adverse effects of the use of recycled aggregates on compressive strength and workability characteristics were also reported by previous studies [45-47]. In particular, CDW-based geopolymer mortar samples activated using 15M NaOH and produced with a 0.6 alkali/binder ratio exhibited severe stability issues, dispersing both in water and under ambient conditions while still in the curing phase, making compressive strength testing impossible. On the other hand, it was observed that the highest compressive strength results were obtained with the use of CS aggregates (43.6 MPa), whereas the specimens exhibiting the minimum compressive strength results were the samples produced using CDW with 3.3 MPa. Even these two examples clearly demonstrate the key role of aggregate type in determining the mechanical performance of geopolymer mortars. In summary, while the superior performance of

crushed stone aggregates can be associated with high adhesion properties, it can be said that achieving acceptable levels of mechanical properties in the case of CDW requires special approaches. On the other hand, Figure 12 also shows that the compressive strengths of GPMs containing SA lie between those containing CS and CDW. This intermediate position necessitated a separate comparison of SA with both aggregates. First, the smooth and rounded grain morphology of SA resulted in a weaker interfacial transition zone (ITZ) compared to CS, resulting in lower compressive strength than CS. In contrast, the lower water absorption of SA compared to CDW allowed the effective activator concentration to be maintained at a constant alkali/binder ratio, resulting in a more continuous gel network and higher strengths compared to CDW. Consequently, it was determined that the observed order of CS > SA > CDW in terms of compressive strength results was consistent with SA forming a weaker ITZ than CS and having lower water absorption than CDW.

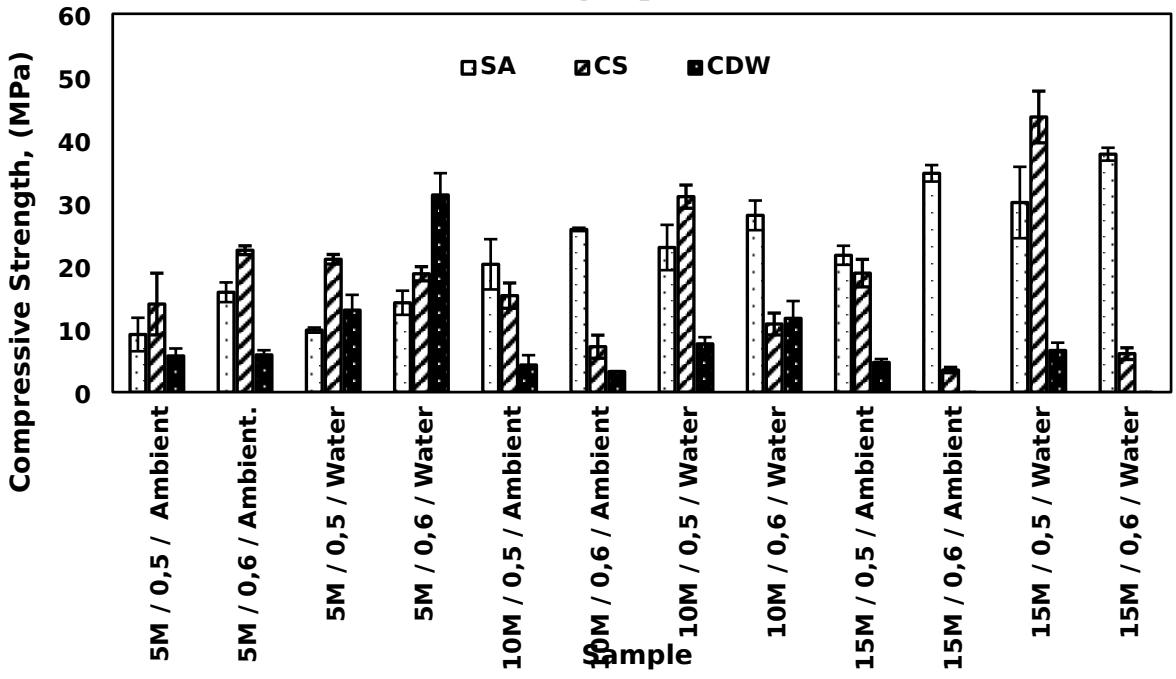


Fig. 12. Effect of aggregate type on compressive strength

3.1.2. Effect of NaOH concentration on compressive strength

ARTICLE IN PRESS

Fig. 13 shows the impacts of three different NaOH concentrations on the compressive strength results of geopolymer mortar samples. As illustrated in Fig. 13, increasing the NaOH concentration in GPM samples produced using SA and CS generally increased the compressive strength values. For instance, in sample groups produced using SA, cured under ambient conditions and using an alkali/binder ratio of 0.6, when the NaOH concentration was increased from 5 M to 15 M, the compressive strength improved by approximately 120%. Similarly, elevating the NaOH concentration from 5 M to 10 M contributed to an increase of approximately 63% in the compressive strength values of the same sample group. It was though that this dramatic improvement can be linked to the enhanced dissolution of aluminosilicate precursors at higher alkalinity levels, leading to denser and more compact gel formation. In parallel with our findings, Huseien et al. (2018) indicated that the mechanical characteristics (compressive, tensile and flexural strengths) of GBFS-based geopolymer crosses increased with increasing NaOH concentration [48]. However, for sample groups produced using SA and CS, the results that the compressive strength values decreased with the higher NaOH concentration were encountered in samples produced using CS and cured in ambient conditions and in water by preferring an alkali/binder ratio of 0.6. For these sample groups, increasing the NaOH concentration from 5 M to 15 M decreased the compressive strength values by about 85% and 68% for the samples subjected to ambient and water curing, respectively. It was speculated that these paradoxical results arise because excessive alkalinity disrupts the gel structure by causing micro cracks. On the other hand, in samples produced using a 0.6 alkali/binder ratio and CDW, compressive strength values of 31.3 MPa were achieved in GPM samples activated with 5 M NaOH, while similar samples activated with 10 M NaOH decreased by 63% to 11.7 MPa. Furthermore, activation with 15 M NAOH resulted in the sample disintegrating during curing in water. It is speculated that these dramatic decreases in compressive strength values in samples produced using CDW, which has a high-water absorption rate, are related to the increased NaOH molarity at a constant alkali/binder ratio

(0.6), which increases solution viscosity and reduces the effective water/solid ratio. Therefore, it is thought that the reduced effective water/solid ratio inhibit particle wetting and ion transport, thereby limiting aluminosilicate dissolution and geopolymer gel formation, resulting in reduced compressive strength values.

All these results further confirm that the optimum alkali concentration must be carefully balanced according to the aggregate type, alkali/binder ratio, and curing conditions to achieve high mechanical properties.

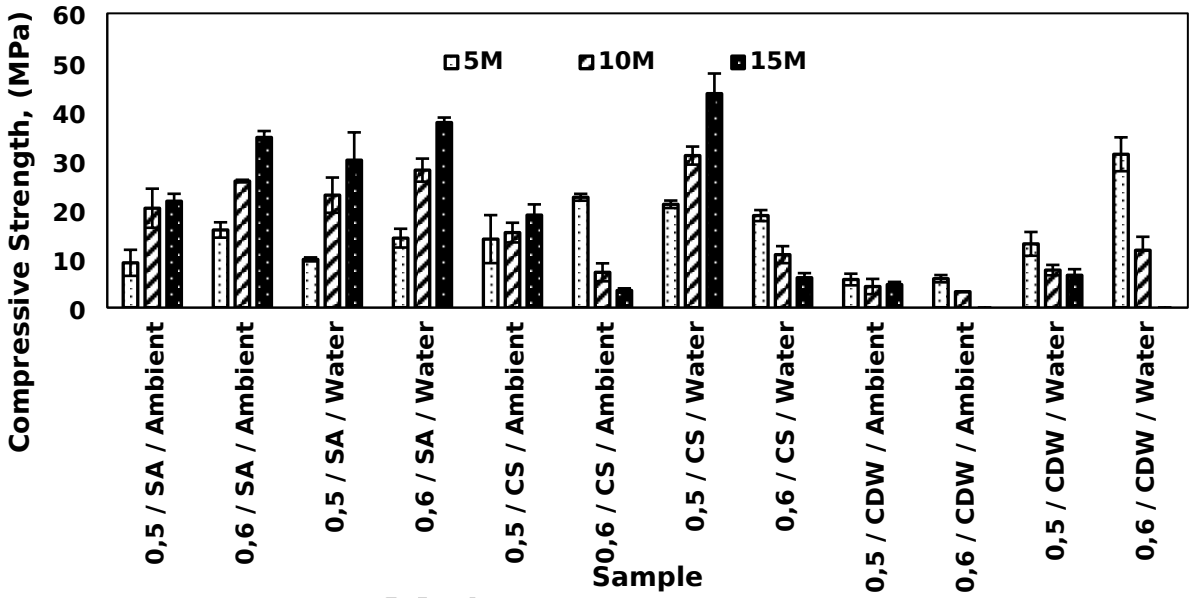


Fig. 13. Effect of NaOH concentration on compressive strength

3.1.3. Effect of applied curing regime on compressive strength

The effects of two different curing regimes applied to geopolymer mortar samples on compressive strength values are shown in Fig. 14. It was observed that in almost all sample groups, the water curing method resulted in considerably higher compressive strength values compared to the ambient curing method. This can be attributed to the use of GBFS as the primary binder material. In GBFS based geopolymer composites, the availability of external water during curing helps to sustain the dissolution of Ca, Si and Al ions, which leads to the formation of a denser and stronger gel structure. With parallel to our findings, Biricik et al. (2021) determined that water curing applied to GBFS-based geopolymer mortar samples had quite positive effects compared to other curing regimes [49]. Additionally,

for sample groups activated using 5 M NaOH, CDW-based and with an alkali/binder ratio of 0.6, the preference of water curing over the ambient curing method increased the 28-day compressive strength records by approximately 430%. This dramatic increase is thought to be due to water curing compensating for moisture loss due to high water absorption encountered in GBFS-based geopolymer composites using porous aggregates such as CDW. Finally, the results obtained revealed that regardless of the aggregate type and alkali concentration used, it is possible to obtain high compressive strength values in GBFS-based geopolymer composites by applying water curing.

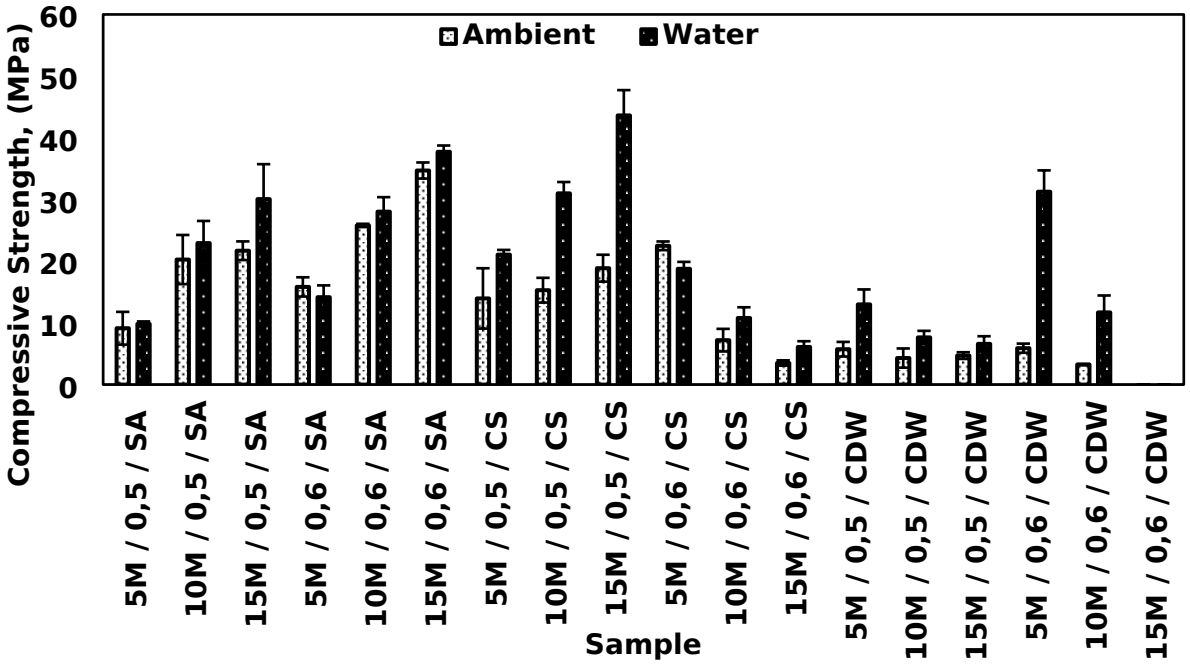


Fig. 14. Effect of applied curing regime on compressive strength

3.1.4. Effect of alkali/binder ratio on compressive strength

The effect of alkali/binder ratio on the 28-day compressive strength values of geopolymer mortar samples produced by taking into account different parameters is shown in Fig. 15. The highest compressive strength results were obtained from samples produced using 0.5 alkali/binder, while the minimum compressive strength values were recorded in samples with 0.6 alkali/binder ratio. Although the minimum and maximum mechanical properties were obtained from different alkali/binder ratios, the results

revealed that the optimum alkali/binder ratio value varied for different NaOH concentrations and aggregate types. For instance, in the ambient cured GPM sample groups and produced with CS aggregates, the optimum alkali/binder ratio was found as 0.6 at 5 M NaOH concentration, while at 15 M NaOH concentration, a lower alkali/binder ratio of 0.5 resulted in higher compressive strength values. These results emphasize that the key factor affecting the compressive strength of geopolymer mortars is the balance between alkali concentration and alkali/binder ratio. It should be emphasized that if the balance is not achieved, excessive alkali content can suppress calcium dissolution and cause a decrease in mechanical properties [50] and similarly, insufficient alkali content can lead to loss of compressive strength [51].

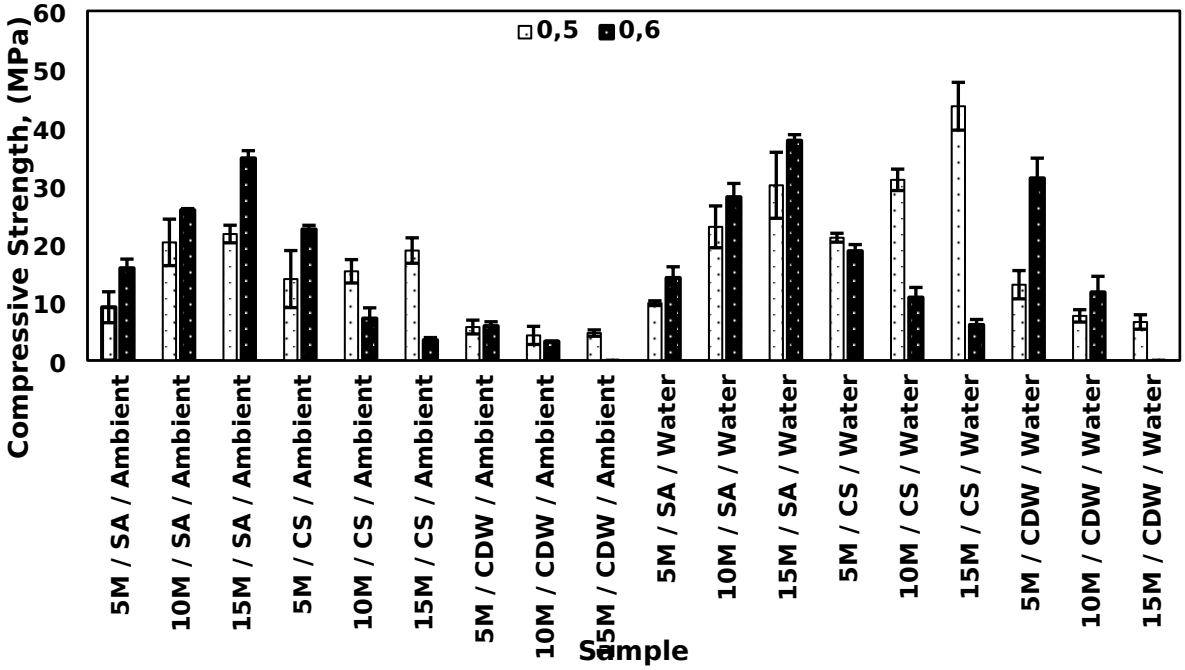


Fig. 15. Effect of alkali/binder ratio on compressive strength

3.2. UPV results of GPM samples

The findings of the UPV tests are given in Fig. 16. As can be seen from Fig. 16, significant relationships were found between compressive strength and UPV values. Namely, maximum UPV values (3521 m/s) were observed in

ARTICLE IN PRESS

the 24th group samples, which were activated with 15 M NaOH, used CS, considered 0.5 alkali/binder ratio and cured in water, where the highest compressive strength values were obtained. UPV test is defined as a process that focuses on phenomena such as fullness and discontinuity in the internal structure of the materials and has the ability to establish a significant relationship with compressive strength. At this point, parallel to our compressive strength test results, it was also confirmed by the UPV test results that the production parameters of the geopolymer mortar samples significantly affected the internal structure. The ability of UPV test results to predict compressive strength has been determined by many researchers in the literature [52, 53]. On the other hand, in parallel with the findings obtained, various studies revealed that the ultra UPV values of concrete are influenced by many factors, including cement type, the existence of micro cracks, the applied curing conditions, the mixture compositions, and the moisture content [52, 54-56]. In addition to these studies conducted on conventional concretes, in another study examining the high temperature performance of GBFS-based GPM specimens, it was underlined that the changes in compressive strength measured under different conditions were also observed in the ultra-sound transmission speed test results and a superior relationship could be established between these two tests [57]. Similarly, Ghosh et al., (2018) investigated the relationship between UPV values and compressive strength results in geopolymer concretes. The findings showed that the relationship between UPV results and compressive strength of concrete was notably influenced by the activator concentration and samples age [58].

ARTICLE IN PRESS

ARTICLE IN PRESS

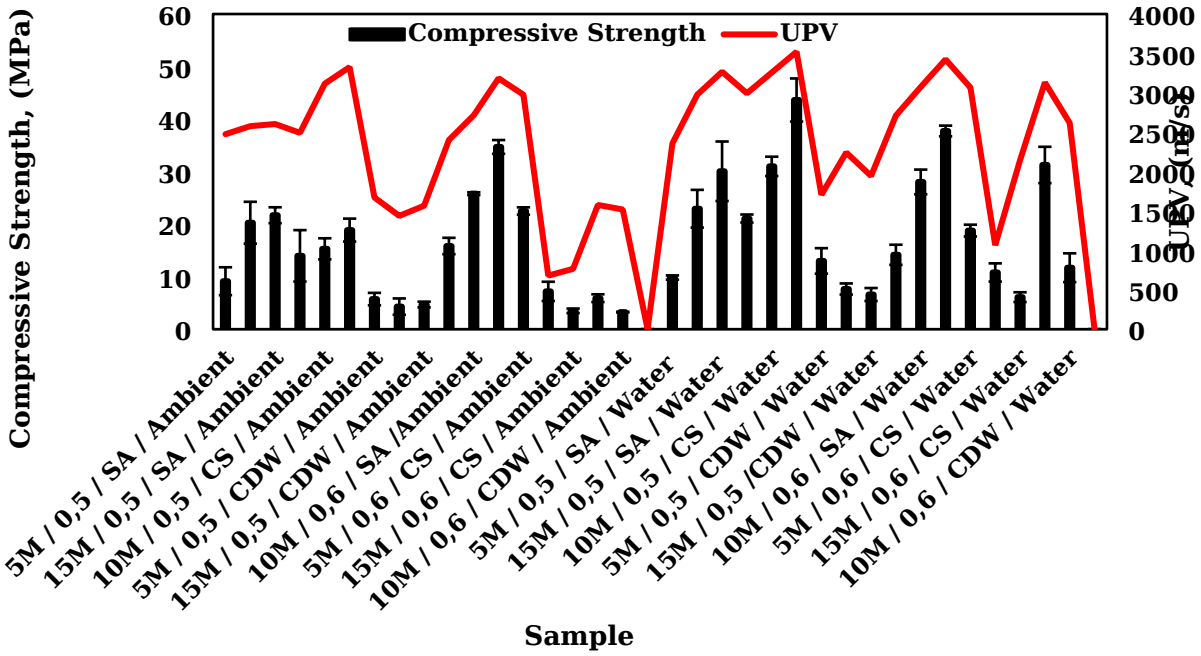


Fig. 16. Relationship between UPV and compressive strength

3.3. Water Absorption

The water absorption values of GPM samples are given in Fig. 17. As presented Fig. 17, the maximum water absorption rates were recorded in the 25th group samples, whereas the minimum water absorption rates were determined to be obtained from the 24th group samples, which have the highest compressive strength. Water absorption values ranging from 3.78% to 26.32% show that the production parameters of geopolymer mortars have very critical effects on permeability. On the other hand, it was determined that the water absorption rates in CDW-based geopolymer mortar samples were quite high. In a previous study, it was reported that the high water absorption properties exhibited by geopolymer mortars produced using CDW were caused by poor interface formation [47]. Similarly, other studies were found that the high water absorption properties of CDW aggregates due to their rough surfaces and irregular shape structures reduce the workability of geopolymer samples [59, 60]. Pedro et al., (2015) underlined that although natural aggregates and CDW aggregates have very different structural properties, the most important difference between these aggregate types is their water absorption properties [61].

In general, as expected, an inverse relationship was proven between the compressive strength results and the water absorption results. Namely, the water absorption values of the samples of groups 7, 8, 9, 15, 16, 17, 26, 27 and 33, where the compressive strength values were quite low, were quite high. While the GPM samples produced using SA led to low water absorption values, the water absorption values of the geopolymer samples produced using CDW were quite high. It should also be noted that the samples produced using 15 M NaOH and CDW at 0.6 alkali/binder ratio were fragmented and the test results could not be obtained. This situation showed that the combination of high alkali/binder ratio, high alkali concentration and CDW served to form a highly porous structure and caused fragmentation without the need for any loading process. On the other hand, in general, increasing NaOH concentration had an effect on the water absorption values in the sample groups produced using SA and CS.

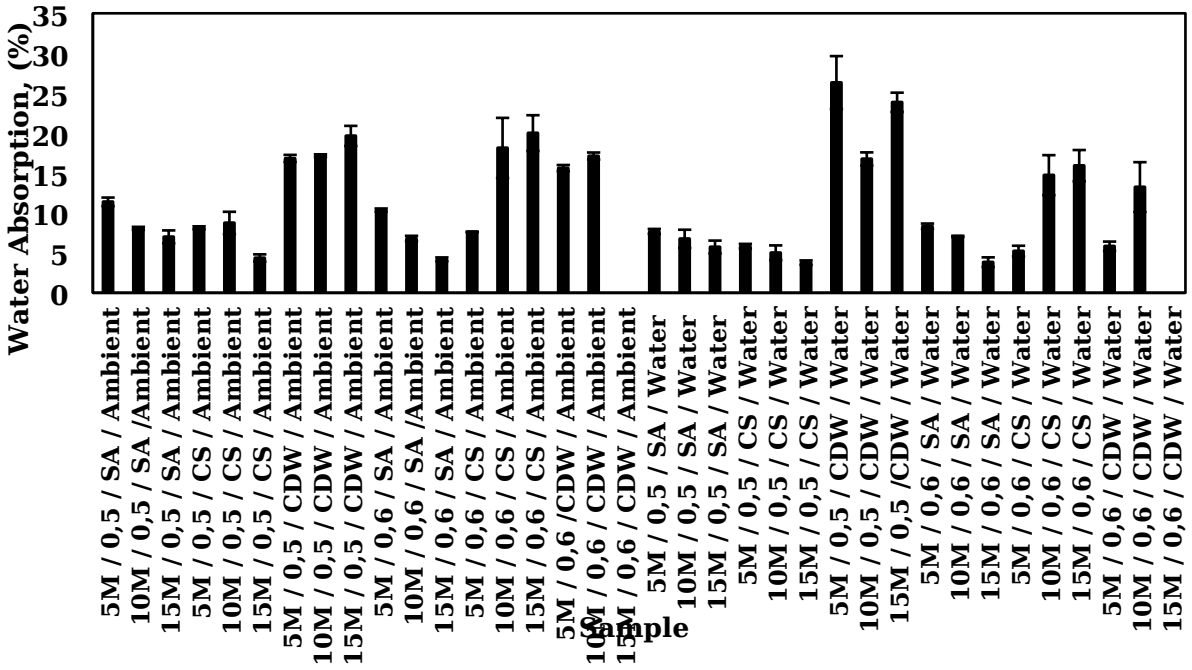


Fig. 17. Water absorption of GPM samples

3.4. Shear Box Test Results

The shear envelopes of a sample group (group 1) formed as a result of the shear box test conducted within the scope of this study are given in Fig. 18 and the shear envelopes of other samples are presented in the appendix.

ARTICLE IN PRESS

The friction angles between the sand-geopolymer mortar determined as a result of the shear box test are presented in Table 7. The friction angle values between geopolymer mortar prepared with different aggregates and sand soil are given in Fig. 19. From this figure, it was determined that aggregate type is one of the main influences on the friction angle. Geopolymer mortars containing CS aggregate appear to achieve the highest interface friction angles. Surface roughness and particle shape were thought to play a critical role in interface behaviour, with angular and rough grains interlocking better and providing higher frictional resistance. However, it was determined that CDW aggregate could provide a higher friction angle in comparison with natural aggregate due to its rough and heterogeneous surface at high molarity (15M). The friction angle values at the interface of sand and geopolymer mortar at 0.5 and 0.6 alkali/binder ratios are given in Fig. 20. According to this figure, higher friction angles were observed as the alkali binder ratio decreased. This situation suggested that the interfacial lubricity increased slightly as the binder ratio increased, thus reducing the friction at the soil-mortar interface. It was also predicted that the occurrence of this behaviour could be associated with the formation of a compact and strong matrix.

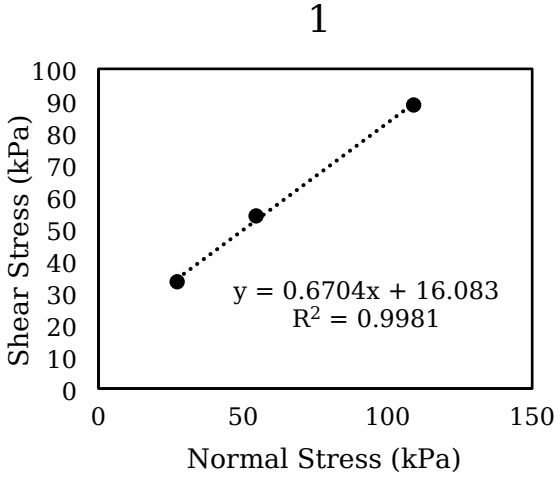


Fig. 18. Mohr–Coulomb failure envelope for sand-geopolymer mortar interface

ARTICLE IN PRESS

Table 7. Interface parameters

Sample Group	Internal Friction Angle
1	33.84
2	35.38
3	31.19
4	43.09
5	43.12
6	37.10
7	32.16
8	35.79
9	38.70
10	31.76
11	32.83
12	37.91
13	41.09
14	37.27
15	37.56
16	30.49
17	24.72
18	38.90
19	38.01
20	35.63
21	36.10
22	38.10
23	40.70
24	35.13
25	36.98
26	31.81
29	35.10
30	38.27

ARTICLE IN PRESS

31	36.80
34	33.56
35	30.90

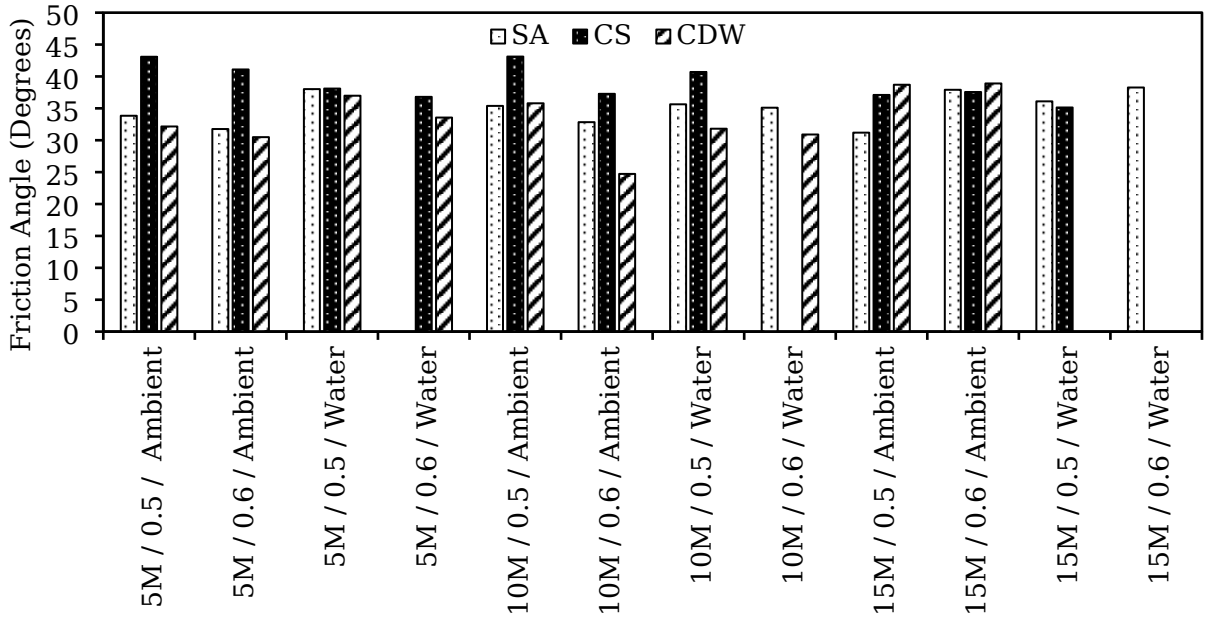


Fig 19. Friction angles at the interface between sand-geopolymer mortar formed with different aggregate types

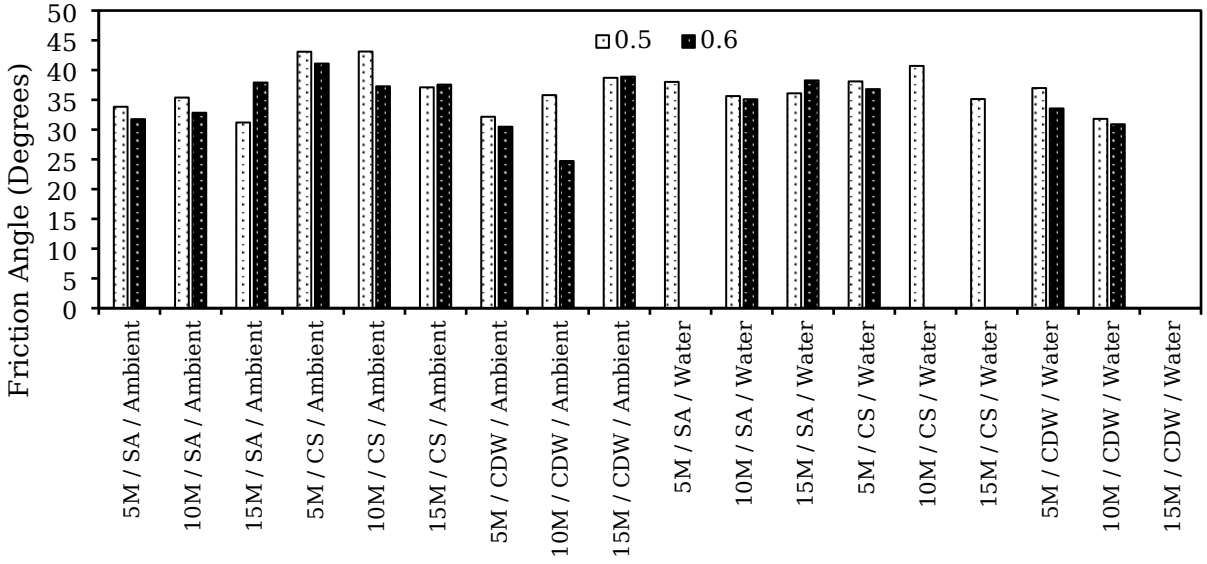


Fig. 20. Friction angles at the interface between sand-geopolymer mortar formed with different molarities

3.5. Numerical Modelling Results

ARTICLE IN PRESS

In order to validate the finite element model, 1, 4 and 7 groups of GPM samples were modelled in light of the experimental findings. The force-displacement curves for each experimental data set were compared with the curves obtained from the numerical models. The load-displacement curve results for samples 1, 4, and 7 are presented in Figs. 21-23**.**

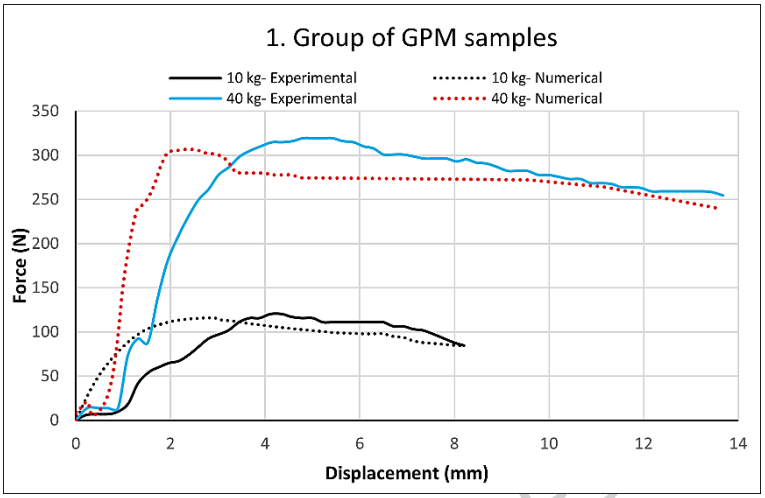


Fig 21. Comparison of force- displacement curves: 1. Group Samples

The experimental data and numerical model show similar behaviour under 10 kg and 40 kg loads, with slight differences as displacement increases. However, the numerical model responds more quickly to dynamic behaviour under 40 kg load, reaching peak force earlier and decreasing curve faster. It is observed that in the numerical model, the force increase occurs more rapidly, the peak force is reached earlier, and the force reduction after sliding is sharper. The key factor behind these differences is that in the numerical model, concrete is modelled as linearly elastic and the sand ground is defined using the Mohr-Coulomb model. In the experimental environment, micro-slips and compressions occur within the ground, causing the force to increase more slowly, whereas in the numerical model, this process is more limited, resulting in the force rising earlier. Additionally, in the experimental system, micro-cracks develop on the concrete surface, causing energy to spread over a wider range, whereas in the numerical model, since the concrete behaves elastically, the stresses reach their maximum more quickly and then show a sudden drop.

ARTICLE IN PRESS

Additionally, while the rearrangement of particles on the experimental surface can sustain friction for a longer period, the numerical model experiences a faster loss of force because the Mohr-Coulomb model transitions to a fully plastic state once the shear limit is reached.

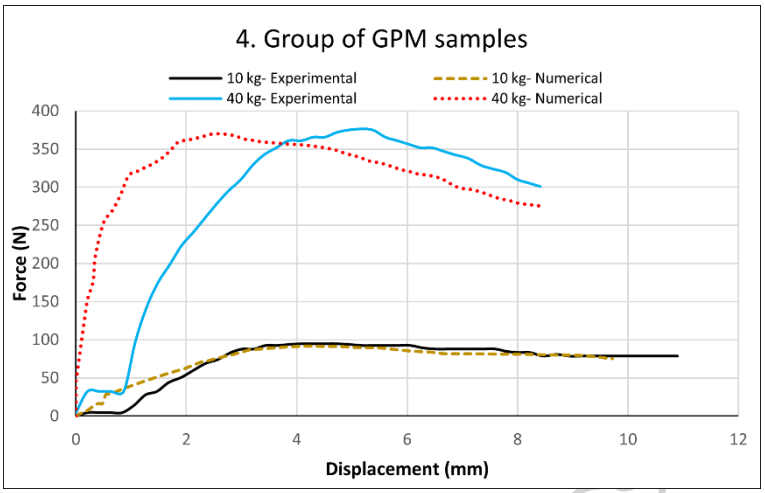


Fig. 22. Comparison of force- displacement curves: 4. Group Samples

For the 4. group of samples, the experimental and numerical graphs generally show similar trends. However, in the numerical model, it is observed that the force initially increases more rapidly, the peak force reaches its maximum earlier compared to the experimental results, and the force reduction after sliding occurs more quickly. The main reason for these differences is that the ground is defined by the Mohr-Coulomb model, while the concrete is defined by the linear elastic model. In the experimental environment, the force increases more slowly due to micro-slips and compressions in the ground, but in the numerical model, this process develops more quickly according to the Mohr-Coulomb criterion. The longer duration of the peak force in the experimental data can be explained by the formation of micro cracks on the concrete surface, causing the energy to spread over a wider range. In contrast, in the numerical model, since concrete is completely elastic, the stresses reach their maximum more quickly and then show a sudden drop. In the post-sliding force reduction, while particles in the experimental ground rearrange themselves to support friction for a while longer, the Mohr-

ARTICLE IN PRESS

Coulomb model transitions to a fully plastic state upon reaching the sliding limit, leading to a faster loss of force.

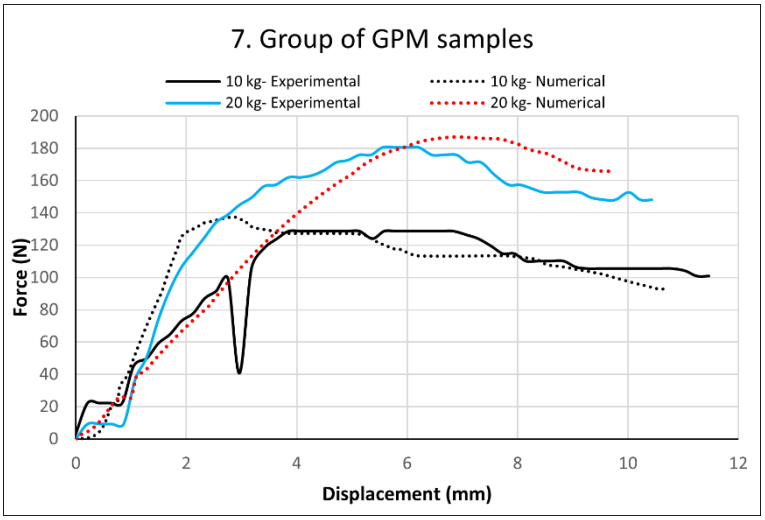


Fig. 23. Comparison of force- displacement curves: 7. Group Samples

For the 7. group of samples, the experimental and numerical force-displacement plots are generally show similar trends. However, in the numerical model, it is observed that the force initially increases more rapidly, the peak force reaches its maximum earlier compared to the experimental data, and the force reduction after sliding occurs more quickly. The main reason for these differences is that the soil is described by the Mohr-Coulomb model, while the concrete is defined by the linear elastic model. In the experimental environment, micro-slips and compressions occur within the ground, causing the force to increase more slowly, whereas in the numerical model, this process is more limited, resulting in an earlier rise in force. The longer duration of the peak force in the experimental data is due to the formation of micro-cracks on the concrete surface, which spreads the energy over a wider period. In the post-sliding force reduction, the Mohr-Coulomb model does not fully reflect the reorganization of the particles in the ground, resulting in a faster decrease in force in the numerical model. Generally, the results obtained from numerical models and experimental data have been obtained similarly. Although there are some inconsistencies due to the preferred material models and certain uncertainties involved in the experiment,

ARTICLE IN PRESS

numerical models can be used in parametric studies with more precise material models.

Conclusions

In this study, the analysis of the shear behavior of GPM samples produced by taking different parameters into consideration at the interface between the sand soil and the sand soil is systematically presented. The following inferences can be made from the data obtained:

- The mechanical performance of GBFS-based geopolymer mortars was largely influenced by variables considered. The use of CS aggregates led to the highest strength values (43.6 MPa) due to superior adhesion properties, whereas the use of CDW resulted in significantly lower compressive strength values unless compensated by optimal liquid content and curing regimes.
- As for the effect of NaOH and alkali/binder ratio, it was observed that these variables should be carefully balanced according to the aggregate type. Regardless of all other variables, it was found that the water curing technique had a consistently positive effect on GBFS-based geopolymer mortar samples.
- Shear box test results demonstrated that aggregate type and alkali/binder ratio significantly affect the friction angle. The decrease in alkali/binder ratio increased the friction angle by producing a denser, stronger matrix. The usage of CS led to higher friction angle values due to its angular and rough morphology. However, satisfactory results were obtained in samples with high alkali concentrations due to the internal structure of CDW being more suitable for geopolymerization and consisting of rough and heterogeneous grains.
- The FEM simulations reproduced the experimental pre-peak hardening and post-peak softening trends but consistently reached peak earlier and softened more sharply. For all FEM analysis, the peak force difference was about −6 to −12% with earlier peaks by

ARTICLE IN PRESS

about 0.5–2.2 mm. Despite these, it can be concluded that the numerical model well replicated the shear behaviour observed in actual direct shear testing, showing strong concordance in force-displacement patterns.

Future research should concentrate on improving numerical models through the incorporation of advanced material laws, consideration of more complex boundary conditions, and further validation investigations under varying loading and environmental conditions. The validated FEM model can provide a solid basis for parametric investigations, facilitating a deeper comprehension of soil-structure interactions, including the effects of recycled aggregates and varying alkali/binder ratios. These efforts would support the development of more reliable geotechnical designs and promote the sustainable use of geopolymer materials in engineering applications.

ARTICLE IN PRESS

Acknowledgements

The authors gratefully acknowledge the financial support of Inonu University (Project ID: 4127).

Author contributions

F.B. Investigation, Validation, Visualization. E.E. Investigation, Visualization, Writing - Original Draft, Conceptualization, Methodology, Validation, Writing – review and editing, Project administration, Supervision, Visualization. T.S. Visualization, Conceptualization, Methodology, Writing – review and editing, Validation. A.Ö. Conceptualization, Writing – review and editing, Supervision, Visualization, Methodology, Validation.

Data availability statement

ARTICLE IN PRESS

The data that support the findings of this study are available from the corresponding author upon reasonable request.

Competing Interests Statement

The authors declare no competing interests.

Funding

The authors will receive funding from the Inonu University Scientific Research Project Unit (Project ID: 4127).

ARTICLE IN PRESS

References

[1] Bamigboye, G. O., Olukanni, D. O., Adedeji, A. A., Ojewumi, M. O., & Jolayemi, K. J. (2018). Experimental and modelling of flexural strength produced from granite-gravel combination in self-compacting concrete. *International. Journal of Civil Engineering Technology*, *9*(7), 437-447.

[2] Mohamad, N., Muthusamy, K., Embong, R., Kusbiantoro, A., & Hashim, M. H. (2022). Environmental impact of cement production and Solutions: A review. *Materials Today: Proceedings*, *48*, 741-746.

[3] Mehta, P. K. (2006). Concrete: Microstructure, Properties, and Materials.

[4] Ren, D., Yan, C., Duan, P., Zhang, Z., Li, L., & Yan, Z. (2017). Durability performances of wollastonite, tremolite and basalt fiber-reinforced metakaolin geopolymer composites under sulfate and chloride attack. *Construction and Building Materials*, *134*, 56-66.

ARTICLE IN PRESS

[5] Kantarci, F., Türkmen, İ., & Ekinci, E. (2021). Improving elevated temperature performance of geopolymer concrete utilizing nano-silica, micro-silica and styrene-butadiene latex. *Construction and Building Materials*, *286*, 122980

[6] He, Z., Shen, A., Lyu, Z., Li, Y., Wu, H., & Wang, W. (2020). Effect of wollastonite microfibers as cement replacement on the properties of cementitious composites: A review. *Construction and Building Materials*, *261*, 119920.

[7] Shi, X. S., Wang, Q., Zhao, X. L., & Collins, F. (2012). Discussion on properties and microstructure of geopolymer concrete containing fly ash and recycled aggregate. *Advanced Materials Research*, *450*, 1577-1583.

[8] Stajanča, M., & Eštoková, A. (2012). Environmental impacts of cement production.

[9] Mohamad, N., Muthusamy, K., Embong, R., Kusbiantoro, A., & Hashim, M. H. (2022). Environmental impact of cement production and Solutions: A review. *Materials Today: Proceedings*, *48*, 741-746.

[10] Pazouki, G. (2022).]Fly ash-based geopolymer concrete's compressive strength estimation by applying artificial intelligence methods. *Measurement*, *203*, 111916.

[11] Davidovits, J. (1991). Geopolymers: inorganic polymeric new materials. *Journal of Thermal Analysis and calorimetry*, *37*(8), 1633-1656.

[12] Manzoor, T., Bhat, J. A., & Shah, A. H. (2024). Performance of geopolymer concrete at elevated temperature− A critical review. Construction and Building Materials, 420, 135578.

[13] Kanagaraj, B., Anand, N., Alengaram, U. J., Praveen, B., & Tattukolla, K. (2022). Performance evaluation on engineering properties and sustainability analysis of high strength geopolymer concrete. *Journal of Building Engineering*, *60*, 105147.

[14] Tayeh, B. A., Zeyad, A. M., Agwa, I. S., & Amin, M. (2021). Effect of elevated temperatures on mechanical properties of lightweight geopolymer concrete. *Case Studies in Construction Materials*, *15*, e00673.

[15] Rahman, S. K., & Al-Ameri, R. (2021). A newly developed self-compacting geopolymer concrete under ambient condition. *Construction and Building Materials*, *267*, 121822.

[16] Chen, K., Wu, D., Zhang, Z., Pan, C., Shen, X., Xia, L., & Zang, J. (2022). Modeling and optimization of fly ash–slag-based geopolymer using response surface method and its application in soft soil stabilization. *Construction and Building Materials*, 315, 125723.

ARTICLE IN PRESS

[17] Geckil, T., Sarici, T., & Aksoy, H. S. (2025). The usability of construction and demolition wastes stabilized using alkali activated fly ash as filler material. Revista de la Construcción. Journal of Construction, 24(2), 428-448.

[18] Sarici, T., Geckil, T., Ok, B., & Aksoy, H. S. (2025). An Investigation of the Usability of Alkali-Activated Blast Furnace Slag-Additive Construction Demolition Waste as Filling Material. Materials, 18(2), 398.

[19] Li, Y., Sun, L., Li, X., & Huang, M. (2022a). Experimental study on the shear mechanical properties of the cemented soil–concrete interface. *European Journal of Environmental and Civil Engineering*, 26(10), 4725-4739.

[20] Janipour, A. K., Mousivand, M., & Bayat, M. (2022). Study of interface shear strength between sand and concrete. *Arabian Journal of Geosciences*, 15(2), 172.

[21] Konkol, J., & Mikina, K. (2021). Some aspects of shear behavior of soft soil–concrete interfaces and its consequences in pile shaft friction modeling. *Materials*, 14(10), 2578.

[22] Zohra, B. F., Fouad, B. A., & Mohamed, C. (2022). Soil-structure interaction interfaces: Literature review. *Arabian Journal of Geosciences*, 15(12), 1130.

[23] Tee, K. F., & Mostofizadeh, S. (2024). Soil–pipe interaction and structural response under static and seismic loading for geopolymer concrete pipes. Innovative Infrastructure Solutions, 9(2), 49.

[24] Haeri, H., Sarfarazi, V., Zhu, Z., Marji, M. F., & Masoumi, A. (2019). Investigation of shear behavior of soil-concrete interface. Smart Structures and Systems, 23(1), 81-90.

[25] Li, D., Shi, C., Ruan, H., & Li, B. (2022). Shear characteristics of soil—concrete structure interaction interfaces. *Applied Sciences*, 12(18), 9145.

[26] Medzvieckas, J., Skuodis, Š., & Sližytė, D. (2019). Numerical analysis of vertical stress distribution in the direct shear box devices.

[27] Dastgerdi, R. H., Khan, A., Kazemi, K., Kowalski, M., Balkaya, M., & Malinowska, A. (2024). Numerical investigation of box shape effects on soil direct shear test. *Rakenteiden Mekaniikka*, 57(2), 65-75.

[28] Moayed, R. Z., Tamassoki, S., & Izadi, E. (2012). Numerical modeling of direct shear tests on sandy clay. *World Academy of Science, Engineering and Technology*, 61, 1093-1097.

[29] Aas, H. (2023). Numerical modeling of direct shear tests of rock joints (Master's thesis, NTNU).

ARTICLE IN PRESS

[30] Zhan, Y. G., Wang, H., & Liu, F. C. (2012). Modeling vertical bearing capacity of pile foundation by using ABAQUS. *Electronic Journal of Geotechnical Engineering*, 17(M), 1855-1865.

[31] Qian, J. G., Gao, Q., Xue, J. F., Chen, H. W., & Huang, M. S. (2017). Soil and ribbed concrete slab interface modeling using large shear box and 3D FEM. *Geomechanical. Engineering*, 12, 295-312.

[32] Tu, Y., Huang, Q., Yao, Q., Fang, Z., Liu, X., & Chai, H. (2025). Shape effect of shear box in large-scale direct shear test for soil-rock mixture. Geomechanics for Energy and the Environment, 100750.

[33] Uysal, F. F.; Bahar, S. Slag Types and Areas of Use. *Trakya University Journal of Engineering Sciences*, 2018, 19(1), 37-52.

[34] Ekinci, E., & Türkmen, İ. (2021). Investigation of the Effect of Different Activator and Raw Material Variables on the Compressive Strength of Geopolymer Dough. *European Journal of Science and Technology*, (24), 169-175.

[35] Sarici, T., & Ozcan, M. (2024). Using geopolymer coated and uncoated geotextile as a hybrid method to improve uplift capacity of screw piles in cohesionless soil. *Alexandria Engineering Journal*, 105, 666-681.

[36] ASTM C109/C109M-21, Standard Test Method for Compressive Strength of Hydraulic Cement Mortars (Using 2-in. or [50 mm] Cube Specimens)1, ASTM International, West Conshohocken, PA. http://www.astm.org

[37] ASTM C 642-06, Standard Test Method for Density, Absorption, and Voids in Hardened Concrete, ASTM International, West Conshohocken, PA. http://www.astm.org

[38] ASTM D3080-04, Standard Test Method for Direct Shear Test of Soils Under Consolidated Drained Conditions, ASTM International, West Conshohocken, PA. http://www.astm.org

[39] Liang, F. Y., Wang, Y. Q., & Han, J. (2011). Numerical analysis of scouring effects on the behavior of pile foundations with the Mohr-Coulomb model. In Condition, Reliability, and Resilience Assessment of Tunnels and Bridges, 82-87.

[40] Sui, C. Y., Shen, Y. S., Wen, Y. M., & Gao, B. (2021). Application of the modified Mohr–Coulomb yield criterion in seismic numerical simulation of tunnels. *Shock and Vibration*, 2021(1), 9968935.

ARTICLE IN PRESS

[41] Wardhono, A., Law, D.W. ve Molyneaux, T.C.K. (2015) Long Term Performance of Alkali Activated Slag Concrete. Journal of Advanced Concrete Technology, 13, 187–192. doi:10.3151/jact.13.187.

[42] Wang, H., Wu, Y., Wang, L., Chen, H. ve Cheng, B. (2021) Properties of a Lightweight Fly Ash–Slag Alkali-Activated Concrete with Three Strength Grades. Applied Sciences, 11(2), 766. doi:10.3390/app11020766.

[43] Thomas, R.J. ve Peethamparan, S. (2015) Alkali-activated concrete: Engineering properties and stress–strain behavior. Construction and Building Materials, 93, 49–56. Erişim: National Science Foundation PAR.

[44] Amer, I., Kohail, M., El-Feky, M. S., Rashad, A., & Khalaf, M. A. (2021). A review on alkali- activated slag concrete. Ain Shams Engineering Journal, 12(2), 1475-1499.

[45] Dimitriou, G., Savva, P., & Petrou, M. F. (2018). Enhancing mechanical and durability properties of recycled aggregate concrete. *Construction and Building Materials*, *158*, 228-235.

[46] Hu, Y., Tang, Z., Li, W., Li, Y., & Tam, V. W. (2019). Physical-mechanical properties of fly ash/GGBFS geopolymer composites with recycled aggregates. *Construction and Building Materials*, *226*, 139-151.

[47] Ekinci, E. (2023). The effects of different production parameters (NaOH concentration, curing regime and replacement ratio of recycled aggregate) on fresh, hardened and elevated temperature performance of geopolymer mortar samples. *Journal of Building Engineering*, *76*, 107052.

[48] Huseien, G. F., Ismail, M., Khalid, N. H. A., Hussin, M. W., & Mirza, J. (2018). Compressive strength and microstructure of assorted wastes incorporated geopolymer mortars: Effect of solution molarity. *Alexandria engineering journal*, *57*(4), 3375-3386.

[49] Biricik, H., Kırgız, M. S., de Sousa Galdino, A. G., Kenai, S., Mirza, J., Kinuthia, J., ... & Khatib, J. (2021). Activation of slag through a combination of NaOH/NaS alkali for transforming it into geopolymer slag binder mortar–assessment the effects of two different Blaine fines and three different curing conditions. *journal of materials research and technology*, *14*, 1569-1584.

[50] Phoo-ngernkham, T., Maegawa, A., Mishima, N., Hatanaka, S., & Chindaprasirt, P. (2015). Effects of sodium hydroxide and sodium silicate

ARTICLE IN PRESS

solutions on compressive and shear bond strengths of FA–GBFS geopolymer. *Construction and Building Materials*, *91*, 1-8.

[51] Qin, T. S., Lim, N. H. A. S., Jun, T. Z., & Ariffin, N. F. (2022). Effect of low molarity alkaline solution on the compressive strength of fly ash based geopolymer concrete. *International Journal of Sustainable Building Technology and Urban Development*, *13*(2), 155-164.

[52] Tan, Y., Yu, H., Mi, R., & Zhang, Y. (2018). Compressive strength evaluation of coral aggregate seawater concrete (CAC) by non-destructive techniques. *Engineering Structures*, *176*, 293-302.

[53] Mata, R., Ruiz, R. O., & Nuñez, E. (2023). Correlation between compressive strength of concrete and ultrasonic pulse velocity: A case of study and a new correlation method. *Construction and Building Materials*, *369*, 130569.

[54] Qasrawi, H. Y. (2000). Concrete strength by combined nondestructive methods simply and reliably predicted. *Cement and concrete research*, *30*(5), 739-746.

[55] Huang, Q., Gardoni, P., & Hurlebaus, S. (2011). Predicting Concrete Compressive Strength Using Ultrasonic Pulse Velocity and Rebound Number. *ACI Materials Journal*, 108 (4).

[56] Tsioulou, O., Lampropoulos, A., & Paschalis, S. (2017). Combined non-destructive testing (NDT) method for the evaluation of the mechanical characteristics of ultra high performance fibre reinforced concrete (UHPFRC). *Construction and Building Materials*, 131, 66-77.

[57] Omer, S. A., Demirboga, R., & Khushefati, W. H. (2015). Relationship between compressive strength and UPV of GGBFS based geopolymer mortars exposed to elevated temperatures. *Construction and Building Materials*, 94, 189-195.

[58] Ghosh, R., Sagar, S. P., Kumar, A., Gupta, S. K., & Kumar, S. (2018). Estimation of geopolymer concrete strength from ultrasonic pulse velocity (UPV) using high power pulser. *Journal of building engineering*, 16, 39-44.

[59] Wang, B., Yan, L., Fu, Q., & Kasal, B. (2021). A comprehensive review on recycled aggregate and recycled aggregate concrete. Resources, *Conservation and Recycling*, 171, 105565.

[60] Kurda, R., de Brito, J., & Silvestre, J. D. (2017). Influence of recycled aggregates and high contents of fly ash on concrete fresh properties. *Cement and Concrete Composites*, 84, 198-213.

[61] Pedro, D., De Brito, J., & Evangelista, L. (2015). Performance of concrete made with aggregates recycled from precasting industry waste:

ARTICLE IN PRESS

influence of the crushing process. *Materials and Structures*, *48*, 3965-3978.

ARTICLE IN PRESS